

Theoretical Study of the ${}^3\text{He}(\mu^-, \nu_\mu) {}^3\text{H}$ Capture

L.E. Marcucci^(a,b), R. Schiavilla^(c,d), S. Rosati^(a,b), A. Kievsky^(b,a), and M. Viviani^(b,a)

(a) *Department of Physics, University of Pisa, I-56100 Pisa, Italy*

(b) *INFN, Sezione di Pisa, I-56100 Pisa, Italy*

(c) *Department of Physics, Old Dominion University, Norfolk, Virginia 23529, USA*

(d) *Jefferson Lab, Newport News, Virginia 23606, USA*

(February 9, 2020)

Abstract

The ${}^3\text{He}(\mu^-, \nu_\mu) {}^3\text{H}$ weak capture is studied using correlated-hyperspherical-harmonics wave functions, obtained from realistic Hamiltonians consisting of the Argonne v_{14} or Argonne v_{18} two-nucleon, and Tucson-Melbourne or Urbana-IX three-nucleon interactions. The nuclear weak charge and current operators have vector and axial-vector components that include one- and two-body contributions. The strength of the leading two-body operator in the axial-vector current is adjusted to reproduce the Gamow-Teller matrix element in tritium β -decay. The calculated total capture rate is in excellent agreement with the most recent experimental determination $1496 \pm 4 \text{ sec}^{-1}$, when the PCAC value is adopted for the induced pseudo-scalar coupling constant g_{PS} . The predictions for the capture rate and angular correlation parameters A_v , A_t , and A_Δ are found to be only very weakly dependent on the model input Hamiltonian. The variation of these observables with g_{PS} and the theoretical uncertainties deriving from the model-dependent procedure used to constrain the axial current are investigated.

21.45.+v, 23.40.-s, 27.10.+h

I. INTRODUCTION

The μ^- weak capture on ^3He can occur through three different hadronic channels:

$$\mu^- + ^3\text{He} \rightarrow ^3\text{H} + \nu_\mu \quad (70\%) , \quad (1.1)$$

$$\mu^- + ^3\text{He} \rightarrow n + d + \nu_\mu \quad (20\%) , \quad (1.2)$$

$$\mu^- + ^3\text{He} \rightarrow n + n + p + \nu_\mu \quad (10\%) . \quad (1.3)$$

The focus of the present work is on the first process. Some of the nuclear physics issues in muon capture have been reviewed recently in Ref. [1].

The reaction (1.1) has been extensively studied through the years, both experimentally and theoretically. Measurements of the total capture rate have been performed since the early sixties [2–4] up to until recently. The latest very precise experimental determination of this observable [5], $1496 \pm 4 \text{ sec}^{-1}$, is consistent with the earlier measurements, the latter having considerably larger uncertainties, however.

Theoretical studies of reaction (1.1) have been carried out within two different frameworks: the so-called “elementary particle method” (EPM) and the fully microscopic approach. The EPM, first developed by Kim and Primakoff [6], is essentially a phenomenological approach, which parameterizes the nuclear (charge-changing) weak current in terms of the trinucleon form factors, in analogy to the nucleon weak current, and then attempts to derive these from other experiments. Within the EPM, it was shown in Ref. [7] that, if the hyperfine structure of the μ^- - ^3He system is taken into account and the direction of the recoiling triton can be detected, there are, in addition to the capture rate, other observables, i.e. angular correlation parameters, which are more sensitive than the capture rate itself to the value of the pseudo-scalar axial coupling constant g_{PS} . Indeed, the possibility of determining g_{PS} from measurements of muon capture observables is one of the motivations for the interest that this process has generated over the years.

In contrast, the fully microscopic approach is based on: i) ^3H and ^3He wave functions as accurate as possible, to reduce uncertainties related to nuclear structure; ii) a realistic model for the nuclear weak current and charge operators. The first microscopic calculation of reaction (1.1) was performed by Peterson in 1968 [8], and was reconsidered and improved by Phillips and collaborators in 1974 [9]. These studies, however, used nuclear wave functions which were approximate, and retained in the nuclear weak transition operators only single-nucleon terms, the impulse approximation (IA).

In the early nineties, the muon capture on ^3He , including the total rate and angular correlation parameters mentioned above, have been extensively investigated, within the fully microscopic framework, by Congleton and Fearing [10], and Congleton and Truhlik [11]. The most significant improvement in these studies, relative to those of the late sixties [8] and early seventies [9], is in the more accurate treatment of the trinucleon wave functions, which have been obtained from a realistic Hamiltonian based on the Argonne v_{14} two-nucleon [12] and Tucson-Melbourne three-nucleon [13] interactions, using the rearrangement coupled-channel method [14].

The study in Ref. [10] used the IA form of the nuclear weak current, and emphasized the need to go beyond single-nucleon contributions for a realistic description of the process. This next step was carried out in Ref. [11], where a model for two-body components in the nuclear weak current was explicitly constructed. The calculated capture rate is in good

agreement with the measured value, although the theoretical prediction suffers from a 2 % uncertainty, which is rather large compared to the experimental error, and mostly arises from poor knowledge of some of the coupling constants and cutoff parameters entering the axial current.

The present work sharpens and updates that of Ref. [11]. Improvements in the modeling of two- and three-nucleon interactions and the nuclear weak current make the re-examination of process (1.1) especially timely. The initial and final state wave functions have been obtained, using the correlated-hyperspherical-harmonics method, from a nuclear Hamiltonian which consists of the Argonne v_{18} two-nucleon [15] and Urbana-IX three-nucleon [16] interactions. To make contact with the study of Ref. [11], however, and to have some estimate of the model dependence of the results, the older Argonne v_{14} two-nucleon and Tucson-Melbourne three-nucleon interaction models have also been used. Both these Hamiltonians reproduce the experimental binding energies and charge radii of the trinucleon systems.

The model for the nuclear weak current, used in the present work and developed in Refs. [17–19], is similar to that of Ref. [11]. The main difference is that the $N\Delta$ -transition coupling constant g_A^* in the axial two-body current due to Δ excitation, the dominant (axial) two-body mechanism, is determined by fitting the measured Gamow-Teller matrix element in tritium β -decay. The inherent model dependence of this procedure has been shown to be very weak in studies of the proton weak captures on ^1H [17] and ^3He [19]. In Ref. [17] predictions for the $^1\text{H}(p, e^+ \nu_e)^2\text{H}$ cross section, obtained with a variety of modern high-quality two-nucleon interactions, differed by significantly less than 1 %, once the coupling constant g_A^* had been fixed as described above within each given model Hamiltonian (for further discussion of this point as well as of the reasons for such a weak model dependence, see Ref. [17]).

A crucial issue, though, remains to be addressed, namely the extent to which the present model for the nuclear weak current is successful in predicting observed weak transitions (note that the cross sections of the weak capture processes mentioned above are not known experimentally). The present work fulfils this need by showing that the calculated rate for μ^- capture on ^3He is in excellent agreement with the measured value.

This manuscript falls into five sections. In Sec. II explicit expressions for the rate and angular correlation parameters are derived in terms of reduced matrix elements of multipole operators, while in Sec. III the model for the weak current is succinctly described. The results are presented and discussed in Sec. IV, and some concluding remarks are given in Sec. V.

II. OBSERVABLES

The muon capture on ^3He is induced by the weak interaction Hamiltonian [20,21]

$$H_W = \frac{G_V}{\sqrt{2}} \int d\mathbf{x} l_\sigma(\mathbf{x}) j^\sigma(\mathbf{x}) , \quad (2.1)$$

where G_V is the Fermi coupling constant, $G_V=1.14939 \times 10^{-5} \text{ GeV}^{-2}$ [22], and l_σ and j^σ are the leptonic and hadronic current densities, respectively. The former is given by

$$l_\sigma(\mathbf{x}) = e^{-i\mathbf{k}_\nu \cdot \mathbf{x}} \bar{u}(\mathbf{k}_\nu, h_\nu) \gamma_\sigma (1 - \gamma_5) \psi_\mu(\mathbf{x}, s_\mu) , \quad (2.2)$$

where $\psi_\mu(\mathbf{x}, s_\mu)$ is the ground-state wave function of the muon in the Coulomb field of the ^3He nucleus, and $u(\mathbf{k}_\nu, h_\nu)$ is the spinor of a muon neutrino with momentum \mathbf{k}_ν , energy E_ν ($=k_\nu$), and helicity h_ν . While in principle the relativistic solution of the Dirac equation could be used, in practice it suffices to approximate

$$\psi_\mu(\mathbf{x}, s_\mu) \simeq \psi_{1s}(x)\chi(s_\mu) \equiv \psi_{1s}(x)u(\mathbf{k}_\mu, s_\mu) \quad \mathbf{k}_\mu \rightarrow 0 \quad , \quad (2.3)$$

since the muon velocity $v_\mu \simeq Z\alpha \ll 1$ (α is the fine-structure constant and $Z=2$). Here $\psi_{1s}(x)$ is the $1s$ solution of the Schrödinger equation and, since the muon is essentially at rest, it is justified to replace the two-component spin state $\chi(s_\mu)$ with the four-component spinor $u(\mathbf{k}_\mu, s_\mu)$ in the limit $\mathbf{k}_\mu \rightarrow 0$. This will allow us to use standard techniques to carry out the spin sum over s_μ at a later stage.

In order to account for the hyperfine structure in the initial system, the muon and ^3He spins are coupled to states with total spin f equal to 0 or 1. The transition amplitude can then be conveniently written as

$$\begin{aligned} T_W(f, f_z; s'_3, h_\nu) &\equiv \langle ^3\text{H}, s'_3; \nu, h_\nu | H_W | (\mu, ^3\text{He}); f, f_z \rangle \\ &\simeq \frac{G_V}{\sqrt{2}} \psi_{1s}^{\text{av}} \sum_{s_\mu, s_3} \left\langle \frac{1}{2} s_\mu, \frac{1}{2} s_3 | f, f_z \right\rangle l_\sigma(h_\nu, s_\mu) \langle ^3\text{H}, s'_3 | j^\sigma(\mathbf{q}) | ^3\text{He}, s_3 \rangle \quad , \end{aligned} \quad (2.4)$$

where

$$l_\sigma(h_\nu, s_\mu) \equiv \bar{u}(\mathbf{k}_\nu, h_\nu) \gamma_\sigma (1 - \gamma_5) u(\mathbf{k}_\mu, s_\mu) \quad , \quad (2.5)$$

and the Fourier transform of the nuclear weak current has been introduced as

$$j^\sigma(\mathbf{q}) = \int d\mathbf{x} e^{i\mathbf{q}\cdot\mathbf{x}} j^\sigma(\mathbf{x}) \equiv (\rho(\mathbf{q}), \mathbf{j}(\mathbf{q})) \quad , \quad (2.6)$$

with the leptonic momentum transfer \mathbf{q} defined as $\mathbf{q} = \mathbf{k}_\mu - \mathbf{k}_\nu \simeq -\mathbf{k}_\nu$. The Bohr radius of the muonic atom in the ground state is about 130 fm, i.e. much larger than the nuclear radius, and it is therefore well justified to factor out $\psi_{1s}(x)$ from the matrix element of $j^\sigma(\mathbf{q})$ between the trinucleon ground states, by approximating it as [20,21]

$$|\psi_{1s}^{\text{av}}|^2 \equiv \mathcal{R} |\psi_{1s}(0)|^2 = \mathcal{R} \frac{(2\alpha m_r)^3}{\pi} \quad , \quad (2.7)$$

where $\psi_{1s}(0)$ denotes the Bohr wave function evaluated at the origin for a point charge $2e$, m_r is the reduced mass of the μ^- - ^3He system, and the factor \mathcal{R} approximately accounts for the finite extent of the nuclear charge distribution [20,21]. The value $\mathcal{R}=0.98$ used here is taken from Ref. [21].

Standard techniques [19,21] are now used to carry out the multipole expansion of the weak charge ($\rho(\mathbf{q})$) and current ($\mathbf{j}(\mathbf{q})$) operators in the general case in which θ is the angle between the spin quantization axis (the $\hat{\mathbf{z}}$ -axis) and the leptonic momentum transfer \mathbf{q} :

$$\langle ^3\text{H}, s'_3 | \rho(\mathbf{q}) | ^3\text{He}, s_3 \rangle = \sqrt{2\pi} \sum_{l=0,1} \sqrt{2l+1} i^l d_{m,0}^l(-\theta) \langle \frac{1}{2} s_3, l m | \frac{1}{2} s'_3 \rangle C_l(q) \quad , \quad (2.8)$$

$$\langle ^3\text{H}, s'_3 | j_z(\mathbf{q}) | ^3\text{He}, s_3 \rangle = -\sqrt{2\pi} \sum_{l=0,1} \sqrt{2l+1} i^l d_{m,0}^l(-\theta) \langle \frac{1}{2} s_3, l m | \frac{1}{2} s'_3 \rangle L_l(q) \quad , \quad (2.9)$$

$$\langle {}^3\text{H}, s'_3 | j_\lambda(\mathbf{q}) | {}^3\text{He}, s_3 \rangle = \sqrt{3\pi} \text{ i} d_{m,-\lambda}^1(-\theta) \langle \frac{1}{2} s_3, l m | \frac{1}{2} s'_3 \rangle [-\lambda M_1(q) + E_1(q)] , \quad (2.10)$$

where $m = s'_3 - s_3$, $\lambda = \pm 1$, and C_l , L_l , E_l and M_l denote the reduced matrix elements (RME's) of the Coulomb (C), longitudinal (L), transverse electric (E) and transverse magnetic (M) multipole operators, as defined in Refs. [19–21]. The $d_{m,m'}^l$ are rotation matrices in the standard notation of Ref. [23]. Since the weak charge and current operators have scalar/polar-vector (V) and pseudo-scalar/axial-vector (A) components, each multipole consists of the sum of V and A terms, having opposite parity under space inversions [19]. Parity and angular-momentum selection rules restrict the contributing RME's to $C_0(V)$, $C_1(A)$, $L_0(V)$, $L_1(A)$, $E_1(A)$ and $M_1(V)$ in the ${}^3\text{He}(\mu^-, \nu_\mu) {}^3\text{H}$ process.

When the triton polarization is not detected, the differential capture rate for the reaction (1.1) is given by

$$d\Gamma = 2\pi \delta(m_\mu + m_\tau - E_\nu - \sqrt{m_t^2 + k_\nu^2}) |\overline{T_W}|^2 \frac{d\mathbf{k}_\nu}{(2\pi)^3} , \quad (2.11)$$

where m_μ , m_τ , and m_t are the rest masses of the muon, ${}^3\text{He}$, and ${}^3\text{H}$, respectively, and the binding energy of the muonic atom has been neglected. Note that the following definition has been introduced:

$$|\overline{T_W}|^2 = \sum_{s'_3, h_\nu} \sum_{f, f_z} P(f, f_z) |T_W(f, f_z; s'_3, h_\nu)|^2 , \quad (2.12)$$

where $P(f, f_z)$ is the probability of finding the $\mu^- {}^3\text{He}$ system in the total-spin state $|f f_z\rangle$. Integrating over the neutrino energy, the differential capture rate reduces to:

$$\frac{d\Gamma}{d(\cos\theta)} = \frac{1}{2} \Gamma_0 \left[1 + A_v P_v \cos\theta + A_t P_t \left(\frac{3}{2} \cos^2\theta - \frac{1}{2} \right) + A_\Delta P_\Delta \right] , \quad (2.13)$$

where the total capture rate Γ_0 reads

$$\Gamma_0 = G_V^2 E_\nu^2 \left(1 - \frac{E_\nu}{m_t} \right) |\psi_{1s}^{\text{av}}|^2 \overline{\Gamma}_0 , \quad (2.14)$$

with $\overline{\Gamma}_0$ denoting the following combination of RME's

$$\overline{\Gamma}_0 \equiv |C_0(V) - L_0(V)|^2 + |C_1(A) - L_1(A)|^2 + |M_1(V) - E_1(A)|^2 . \quad (2.15)$$

The angular correlation parameters A_v , A_t and A_Δ are given by:

$$A_v = 1 + \frac{1}{\overline{\Gamma}_0} \left[2 \text{Im}[(C_0(V) - L_0(V))(C_1(A) - L_1(A))^*] - |M_1(V) - E_1(A)|^2 \right] , \quad (2.16)$$

$$\begin{aligned} A_t = & \frac{4}{3} \frac{1}{\overline{\Gamma}_0} \left[\text{Im}[(C_0(V) - L_0(V))(C_1(A) - L_1(A))^*] \right. \\ & - \frac{1}{\sqrt{2}} \text{Im}[(C_0(V) - L_0(V))(M_1(V) - E_1(A))^*] \\ & \left. + \frac{1}{\sqrt{2}} \text{Re}[(C_1(A) - L_1(A))(M_1(V) - E_1(A))^*] - \frac{1}{2} |M_1(V) - E_1(A)|^2 \right] , \end{aligned} \quad (2.17)$$

$$\begin{aligned}
A_\Delta = & \frac{2}{3} \frac{1}{\bar{\Gamma}_0} \left[\sqrt{2} \text{Im} \left[(C_0(V) - L_0(V))(M_1(V) - E_1(A))^* \right] \right. \\
& - \sqrt{2} \text{Re} \left[(C_1(A) - L_1(A))(M_1(V) - E_1(A))^* \right] \\
& \left. + \text{Im} \left[(C_0(V) - L_0(V))(C_1(A) - L_1(A))^* \right] - \frac{1}{2} |M_1(V) - E_1(A)|^2 \right]. \quad (2.18)
\end{aligned}$$

Finally, the coefficients P_v , P_t and P_Δ are linear combinations of the probabilities $P(f, f_z)$, and are defined as [7,10]

$$\begin{aligned}
P_v &= P(1, 1) - P(1, -1), \\
P_t &= P(1, 1) + P(1, -1) - 2 P(1, 0), \\
P_\Delta &= P(1, 1) + P(1, -1) + P(1, 0) - 3 P(0, 0) = 1 - 4 P(0, 0). \quad (2.19)
\end{aligned}$$

Therefore, P_v and P_t are proportional to the vector and tensor polarizations of the $f=1$ state, respectively, while P_Δ indicates the deviation of the $f=0$ population density from its statistical factor 1/4. Because of the small energy splitting between the $f=0$ and $f=1$ hyperfine states (1.5 eV) compared to the μ^- He binding energy, and hence small deviation of $P(f, f_z)$ from its statistical value, it is not yet clear how a direct measurement of the angular correlation parameters could be experimentally performed [1,10].

III. THE WEAK CHARGE AND CURRENT OPERATORS

An exhaustive description of the model for the nuclear weak current has been recently given in Ref. [19]. Here only its main features are summarized.

The nuclear weak current consists of vector and axial-vector parts, with corresponding one- and two-body components. The weak vector current is constructed from the isovector part of the electromagnetic current, in accordance with the conserved-vector-current (CVC) hypothesis. One important difference between the present calculations and those reported in Ref. [19] is that the leptonic four-momentum transfer is not negligible, but in fact close to the muon rest-mass. Consequently, electromagnetic form factors need to be included in the expressions listed in Ref. [19]. The parameterization used for these (see, for example, Ref. [24]) reproduces available eN elastic scattering data.

The one-body terms in the axial charge and current operators have the standard expressions [19] obtained from the non-relativistic reduction of the covariant single-nucleon current, and retain terms proportional to $1/m^2$, m being the nucleon mass. Again, because the leptonic momentum transfer involved in muon capture is not negligible, axial and induced pseudo-scalar form factors need to be included. These are parameterized as

$$g_A(q_\sigma^2) = \frac{g_A}{(1 + q_\sigma^2/\Lambda_A^2)^2}, \quad (3.1)$$

$$g_{PS}(q_\sigma^2) = -\frac{2m_\mu m}{m_\pi^2 + q_\sigma^2} g_A(q_\sigma^2), \quad (3.2)$$

where q_σ^2 is the four-momentum transfer. The axial-vector coupling constant g_A is taken to be [25] 1.2654 ± 0.0042 , by averaging values obtained from the beta asymmetry in the decay of

polarized neutrons and the half-lives of the neutron and super-allowed $0^+ \rightarrow 0^+$ transitions. The value for the cutoff mass Λ_A is found to be approximately $1 \text{ GeV}/c^2$ from an analysis of pion electro-production data [26] and measurements of the reaction $p(\nu_\mu, \mu^+)n$ [27]. The q_σ^2 -dependence of g_{PS} is obtained in accordance with the partially-conserved-axial-current hypothesis (PCAC), by assuming pion-pole dominance and the Goldberger-Treiman relation [20,21], m_π here indicates the pion mass.

Some of the two-body axial-current operators are derived from π - and ρ -meson exchanges and the $\rho\pi$ -transition mechanism. These mesonic operators, first obtained in a systematic way in Ref. [28], give rather small contributions [19]. The two-body weak axial-charge operator includes a pion-range term, which follows from soft-pion theorem and current algebra arguments [29,30], and short-range terms, associated with scalar- and vector-meson exchanges. The latter are obtained consistently with the two-nucleon interaction model, following a procedure [31] similar to that used to derive the corresponding weak vector-current operators [19].

The dominant two-body axial current operator, however, is that due to Δ -isobar excitation [17,19]. Since the $N\Delta$ transition axial-vector coupling constant g_A^* is not known experimentally, the associated contribution suffers from a large model dependence. To reduce it [17,19], the coupling constant g_A^* has been adjusted to reproduce the experimental value of the Gamow-Teller matrix element in tritium β decay, $\text{GT}^{\text{EXP}} = 0.957 \pm 0.003$ [17].

The Δ -excitation operator used here is that derived, in the static Δ approximation, using first-order perturbation theory. This approach is considerably simpler than that adopted in Ref. [19], where the Δ degrees of freedom were treated non-perturbatively, by retaining them explicitly in the nuclear wave functions [32]. However, it is important to emphasize [19] that the results obtained within the perturbative and non-perturbative schemes are typically within 1 % of each other, once g_A^* is fixed, independently in the perturbative and non-perturbative calculations, to reproduce the experimentally known Gamow-Teller matrix element. The values for the ratio g_A^*/g_A determined in the present study are listed in Table I for the four different combinations of interaction models. The experimental error on GT^{EXP} is responsible for the 8–9 % uncertainty in g_A^* .

IV. RESULTS

In this section results for the ${}^3\text{He}(\mu^-, \nu_\mu){}^3\text{H}$ capture process are reported. The trinucleon wave functions have been obtained from a realistic Hamiltonian consisting of the Argonne v_{18} (AV18) [15] two-nucleon and Urbana IX (UIX) [16] three-nucleon interactions. To compare with earlier predictions [10,11] for the same process, and to have some estimate of the model dependence, the older Argonne v_{14} (AV14) [12] two-nucleon and Tucson-Melbourne (TM) [13] three-nucleon interactions have also been used. Note that both the UIX and TM interactions have been adjusted to reproduce the triton binding energy. Finally, to investigate the effect of the three-nucleon interaction, predictions for muon-capture observables have been made by including only two-nucleon interactions (AV14 or AV18) in the Hamiltonian models.

The three-body bound-state problem has been solved with the correlated-hyperspherical-harmonics (CHH) method, as described in Refs. [33,34]. It consists essentially in expanding the wave function on the CHH basis, and in determining variationally the expansion coef-

ficients by applying either the Rayleigh-Ritz or Kohn variational principles, depending on whether bound- or scattering-state solutions are sought.

The ^3H and ^3He binding energies are listed in Table II for the different model Hamiltonians employed in the present work. They are obtained including only the isospin 1/2 components of the wave functions. These results, which are very accurate (the uncertainty is of the order of one keV), are in excellent agreement with the values calculated using other techniques (for a review, see Ref. [35]).

Results for the capture rate Γ_0 and angular correlation parameters A_v , A_t , and A_Δ , defined in Eqs. (2.14)–(2.18), are presented in Table III. The uncertainty (in parenthesis) in the predicted values is due to the uncertainty in the determination of the $N\Delta$ transition coupling constant g_A^* (see Sec. III and Table I). The latter reflects the experimental error in the Gamow-Teller matrix element of tritium β -decay.

Inspection of Table III shows that the theoretical determination of the total capture rate, when the AV18/UIX and AV14/TM Hamiltonian models are used, is in excellent agreement with the recent experimental result [5], $1496 \pm 4 \text{ sec}^{-1}$. Furthermore, the model dependence in the calculated observables is very weak: the AV18/UIX and AV14/TM results differ by less than 0.5 %. The agreement between theory and experiment and the weak model dependence mentioned above reflect, to a large extent, the fact that both the AV18/UIX and AV14/TM Hamiltonian models reproduce: i) the experimental binding energies as well as the charge and magnetic radii [24] of the trinucleons; ii) the Gamow-Teller matrix element in tritium β -decay. In this respect, it is interesting to note that the capture rates predicted by the AV18 and AV14 Hamiltonian models are about 3 % smaller than the experimental value, presumably because of the under-prediction of the binding energies and consequent over-prediction of the radii. This makes the relevant nuclear form factors, entering into the expression for the rate Γ_0 , smaller at the momentum transfer of interest, $q \simeq 103 \text{ MeV}/c$, than they would be otherwise. To study how the rate Γ_0 scales with the triton binding energy, we have repeated the calculation using CHH wave functions obtained with a modified AV14/TM Hamiltonian model, which gives for the ^3H and ^3He binding energies 9.042 and 8.349, respectively. The result for the rate Γ_0 is $1517 \pm 8 \text{ sec}^{-1}$, while the angular correlation parameters are very close to the AV14/TM values listed in Table III. Therefore, the rate Γ_0 scales approximately linearly with the trinucleon binding energy.

The contributions of the different components of the weak current and charge operators to the observables and to the RME's of the contributing multipoles are reported for the AV18/UIX model in Tables IV and V, respectively. The coupling constant g_A^* has been set equal to the central value of 1.17 g_A (see Table I). The notation in Tables IV and V is as follows. The column labeled “One-body” lists the contributions associated with the one-body terms of the vector and axial charge and current operators, including relativistic corrections proportional to $1/m^2$. These are essentially the operators given in Eqs. (4.5), (4.8), (4.10), and (4.11) of Ref. [19], suitably modified by the inclusion of nucleon form factors, as explained in Sec. III. Note, however, that the present study retains, in addition, the Darwin-Foldy term in the vector charge and the term

$$\rho_{i,PS}^{(1)}(\mathbf{q}; A) = -\frac{g_{PS}}{2m m_\mu} (m_\mu - E_\nu) (\boldsymbol{\sigma}_i \cdot \mathbf{q}) \tau_{i,-} , \quad (4.1)$$

from the induced pseudo-scalar contribution, in the axial charge (notations as in Ref. [19]).

The column labeled ‘‘Mesonic’’ lists the contributions from two-body vector and axial charge and current operators, associated with pion- and vector-meson-exchanges, namely those of Eqs. (4.16)–(4.17), (4.30)–(4.31), (4.32)–(4.34), and (4.35)–(4.37) of Ref. [19], again modified by the inclusion of form factors. Finally, the column labeled ‘‘ Δ ’’ lists the contributions arising from Δ excitation. The associated operators, as mentioned earlier in Sec. III, are obtained using perturbation theory and the static Δ approximation as in Eqs. (4.44), (4.48), (4.50) and (4.52) of Ref. [19].

Note that in Table V the values for the RME $L_0(V)$ have not been listed, since the charge and longitudinal multipole operators of the weak vector current, denoted respectively as $C_{ll_z}(q; V)$ and $L_{ll_z}(q; V)$, are related via CVC as [19]

$$L_{ll_z}(q; V) = -\frac{1}{q} [H, C_{ll_z}(q; V)] . \quad (4.2)$$

In turn, this implies the following proportionality between the corresponding RME’s $C_0(V)$ and $L_0(V)$, $L_0(V) = (m_\tau - m_t - q^2/2m_t) C_0(V)/q$, or $L_0(V) \simeq -0.024 C_0(V)$ for $q \simeq 103$ MeV/ c .

Among the observables, Γ_0 and A_Δ are the most sensitive to two-body contributions in the weak current. These are in fact crucial for reproducing the experimental capture rate, see Table IV. Inspection of Table V shows that two-body contributions are significant in the RME’s $M_1(V)$, $L_1(A)$, and $E_1(A)$, but negligible in $C_0(V)$. The $C_0(V)$ and $M_1(V)$ RME’s are related by CVC to the corresponding RME’s of the isovector part of the electromagnetic current, since

$$\mathbf{j}_-(\mathbf{q}; V) = [T_-, \mathbf{j}_{iv}(\mathbf{q}; \gamma)] , \quad (4.3)$$

where $\mathbf{j}_-(\mathbf{q}; V)$ is charge-lowering weak vector current, $\mathbf{j}_{iv}(\mathbf{q}; \gamma)$ is the isovector part of the electromagnetic current, and T_- is the (total) isospin-lowering operator. A similar relation holds between the electromagnetic charge operator and its weak vector counterpart. Thus, if ${}^3\text{He}$ and ${}^3\text{H}$ were truly members of an isospin doublet, then the $C_0(V)$ and $M_1(V)$ RME’s would just be proportional to the isovector combination of the trinucleon charge and magnetic form factors. Of course, electromagnetic terms and isospin-symmetry-breaking strong-interaction components in the nuclear potentials spoil this property. For example, the AV18/UIX model predicts for the isovector RME’s $C_{0,iv}(\gamma)$ and $M_{1,iv}(\gamma)$ at $q \simeq 103$ MeV/ c the values 0.3250 and -0.1385 (0.3254 and -0.1113 in impulse approximation), respectively.

The $C_1(A)$ RME is about two orders of magnitude smaller than the leading RME’s, as expected on the basis of the following naive argument. The one-body axial charge density operator can be written approximately as (the notation is that of Ref. [19])

$$\rho_i^{(1)}(\mathbf{x}; A) = -\frac{g_A}{2m} \tau_{i,-} \boldsymbol{\sigma}_i \cdot [\mathbf{p}_i, \delta(\mathbf{x} - \mathbf{r}_i)]_+ \simeq i \frac{g_A}{2m} \tau_{i,-} \boldsymbol{\sigma}_i \cdot \nabla_i \delta(\mathbf{x} - \mathbf{r}_i) , \quad (4.4)$$

where the term proportional to \mathbf{p}_i has been neglected, and the identity $[A, B]_+ = [A, B]_- + 2BA$ has been used. Here $[A, B]_\pm$ denote the anticommutator (+) and commutator (−), respectively. We have also neglected the induced pseudo-scalar contribution. The one-body axial current density (its leading term) is

$$\mathbf{j}_{i,\text{NR}}^{(1)}(\mathbf{x}; A) = -g_A \tau_{i,-} \boldsymbol{\sigma}_i \delta(\mathbf{x} - \mathbf{r}_i) , \quad (4.5)$$

and insertion of the approximation (4.4) and Eq. (4.5) into the expressions for the charge and longitudinal multipole operators leads to the following relation between the associated RME's: $C_1(A) \simeq -(q/2m) L_1(A)$, which, for $q \simeq 103$ MeV/c, gives $C_1(A) \simeq -0.055 L_1(A)$, i.e. the correct sign and order of magnitude obtained in the calculation.

Lastly, it is interesting to note that the contribution from the pion-exchange axial charge operator, which would be expected to be dominant among the two-body contributions to $C_1(A)$, is in fact negligible. The operator structure of the corresponding $C_1(A)$ multipole is such that it cannot connect the dominant S-wave components in the ${}^3\text{He}$ and ${}^3\text{H}$ wave functions, and the associated matrix element is therefore highly suppressed.

In order to compare with the results of Ref. [10], the capture rate and angular correlation parameters have been calculated with the CHH wave functions corresponding to the AV14/TM Hamiltonian, and with a model for the nuclear weak current including only one-body terms. The values for the coupling constants and form factors entering the expressions for the charge and current operators have been taken from Ref. [10]. The comparison between the present and earlier predictions is shown in Table VI: there is satisfactory agreement between the two calculations. The remaining 1–3 % differences can presumably be explained as follows: i) the nuclear wave functions have been obtained with an AV14/TM Hamiltonian model with slightly different cutoff parameters [36]; ii) the weak one-body operators in Ref. [10] include some of the next-to-next-to-leading orders in the non-relativistic expansion of the covariant single-nucleon current, proportional to $1/m^3$, these are ignored in the present calculation; iii) the numerical evaluation of the required matrix elements is performed with different techniques. Here, Monte Carlo methods based on the Metropolis *et al.* algorithm [37] have been used. Typically, the statistical error on the calculated capture rate is less than 0.05 %.

The results listed in Table III, column labeled “AV14/TM”, are also in good agreement with those of Table IX of Ref. [11], although the treatment of the short-range behavior of the two-body terms in the weak current as well as the values for the vector and axial form factors, coupling constants, etc. in Ref. [11] are slightly different from those adopted in the present work. It is important to emphasize, though, that the present model for the weak current reproduces well the available experimental data: i) the isovector component of the electromagnetic current, which by CVC is related to the weak vector current, leads to predictions for the isovector combination of the charge and magnetic form factors of ${}^3\text{He}$ and ${}^3\text{H}$ in excellent agreement with the measured values [24] up to momentum transfer of $\simeq 3$ fm $^{-1}$; ii) the two-body axial current operators are constrained to reproduce the Gamow-Teller matrix element in tritium β -decay.

To test the sensitivity of all the muon capture observables to g_{PS} , these have been calculated, using the AV18/UIX CHH wave functions, for several different values of g_{PS} . The variation of each observable in terms of its deviation from the reference prediction obtained adopting g_{PS}^{PCAC} , is displayed in Fig. 1. The angular correlation parameters, in particular A_t and A_Δ , are more sensitive to changes in g_{PS} than the total capture rate, as first pointed out in Ref. [7]. A precise measurement of these polarization observables could therefore be useful to ascertain the extent to which g_{PS} deviates from its PCAC value.

Finally, by enforcing perfect agreement between the experimental and theoretical values, taken with their uncertainties, for the total capture rate Γ_0 , it is possible to obtain an

estimate for the range of values allowed for g_{PS} . This procedure gives $g_{PS}/g_{PS}^{\text{PCAC}} = 0.98 \pm 0.06$. This 6 % uncertainty is smaller than that found in previous studies [10,11,38].

V. SUMMARY AND CONCLUSIONS

Muon capture observables for the process ${}^3\text{He}(\mu^-, \nu_\mu){}^3\text{H}$ have been calculated with very accurate CHH wave functions corresponding to realistic Hamiltonians, the AV18/UIX and AV14/TM models, and with a nuclear weak current consisting of vector and axial-vector parts with one- and two-body terms. The conserved-vector-current hypothesis has been used to derive the weak vector charge and current operators from the isovector electromagnetic counterparts, while the axial current has been constructed to reproduce the measured Gamow-Teller matrix element of ${}^3\text{H}$ β -decay. It should be emphasized that the model adopted for the electromagnetic current provides an excellent description of the ${}^3\text{He}$ and ${}^3\text{H}$ charge and magnetic form factors [24] at low and medium values of momentum transfers.

The predicted total capture rate is in excellent agreement with the experimental value, and has been found to have only a weak model dependence: the AV18/UIX and AV14/TM results differ by less than 0.5 %. The weak model dependence can be traced back to the fact that both Hamiltonians reproduce the binding energies, charge and magnetic radii of the trinucleons, and the Gamow-Teller matrix element in tritium β -decay.

It is important to note that, if the contributions associated with two-body terms in the axial current were to be neglected, the predicted capture rate would be 1316 (1318) sec^{-1} with AV18/UIX (AV14/TM), and so two-body mechanisms are crucial for reproducing the experimental value. The present work demonstrates that the procedure adopted for constraining these two-body contributions leads to a consistent description of available experimental data on weak transitions in the three-body systems. It also corroborates the robustness of our recent predictions for the cross sections of the proton weak captures on ${}^1\text{H}$ [17] and ${}^3\text{He}$ [18,19], which were obtained with the same model for the nuclear weak current.

Finally, it would be interesting to study the ${}^3\text{He}(\mu^-, \nu_\mu)nd$ and ${}^3\text{He}(\mu^-, \nu_\mu)nnp$ processes, both of which have been investigated experimentally in Ref. [39] and theoretically in Ref. [40]. Since the CHH method is able at present to solve for three- and four-body bound and scattering states [41–43], the study of these two processes is also possible. Work along these lines is vigorously being pursued.

ACKNOWLEDGMENTS

The authors wish to thank E. Truhlik for useful discussions. The work of R.S. is supported by the U.S. Department of Energy contract number DE-AC05-84ER40150 under which the Southeastern Universities Research Association (SURA) operates the Thomas Jefferson National Accelerator Facility. Some of the calculations were made possible by grants of computing time from the National Energy Research Supercomputer Center in Livermore.

REFERENCES

- [1] D.F. Measday, Phys. Rep. **354**, 243 (2001).
- [2] I.V. Folomkin *et al.*, Phys. Lett. **3**, 229 (1963).
- [3] L.B. Auerbach *et al.*, Phys. Rev. **138**, B127 (1965).
- [4] D.R. Clay, J.W. Keuffel, R.L. Wagner, and R.M. Edelstein, Phys. Rev. **140**, B587 (1965).
- [5] P. Ackerbauer *et al.*, Phys. Lett. B **417**, 224 (1998).
- [6] C.W. Kim and H. Primakoff, Phys. Rev. **140**, B566 (1965).
- [7] W.-Y.P. Hwang, Phys. Rev. C **17**, 1799 (1978).
- [8] E.M. Peterson, Phys. Rev. **167**, 971 (1968).
- [9] A.C. Phillips, F. Roig, and J. Ros, Nucl. Phys. A **237**, 493 (1974).
- [10] J.G. Congleton and H.W. Fearing, Nucl. Phys. A **552**, 534 (1992).
- [11] J.G. Congleton and E. Truhlik, Phys. Rev. C **53**, 956 (1995).
- [12] R.B. Wiringa, R.A. Smith, and T.A. Ainsworth, Phys. Rev. C **29**, 1207 (1984).
- [13] S.A. Coon *et al.*, Nucl. Phys. A **317**, 242 (1979).
- [14] H. Kameyama, M. Kamimura, and Y. Fukushima, Phys. Rev. C **40**, 974 (1989); M. Kamimura and H. Kameyama, Nucl. Phys. A **508**, 17c (1990).
- [15] R.B. Wiringa, V.G.J. Stoks, and R. Schiavilla, Phys. Rev. C **51**, 38 (1995).
- [16] B.S. Pudliner, V.R. Pandharipande, J. Carlson, and R.B. Wiringa, Phys. Rev. Lett. **74**, 4396 (1995).
- [17] R. Schiavilla *et al.*, Phys. Rev. C **58**, 1263 (1998).
- [18] L.E. Marcucci, R. Schiavilla, M. Viviani, A. Kievsky, and S. Rosati, Phys. Rev. Lett. **84**, 5959 (2000).
- [19] L.E. Marcucci *et al.*, Phys. Rev. C **63**, 015801 (2001).
- [20] J.D. Walecka, in *Muon Physics; Weak Interactions*, edited by V.W. Hughes and C.S. Wu (Academic Press, New York, 1975), p. 114.
- [21] J.D. Walecka, *Theoretical Nuclear and Subnuclear Physics* (Oxford University Press, New York, 1995).
- [22] J.C. Hardy, I.S. Towner, V.T. Koslowsky, E. Hagberg, and H. Schmeing, Nucl. Phys. A **509**, 429 (1990).
- [23] A.R. Edmonds, *Angular Momentum in Quantum Mechanics* (Princeton University Press, Princeton, 1957).
- [24] L.E. Marcucci, D.O. Riska, and R. Schiavilla, Phys. Rev. C **58**, 3069 (1998).
- [25] E. Adelberger *et al.*, Rev. Mod. Phys. **70**, 1265 (1998).
- [26] E. Amaldi, S. Fubini, and G. Furlan, in *Electroproduction at Low Energy and Hadron Form Factors*, Springer Tracts in Modern Physics No. 83, 1 (1979).
- [27] T. Kitagaki *et al.*, Phys. Rev. D **28**, 436 (1983).
- [28] M. Chemtob and M. Rho, Nucl. Phys. A **163**, 1 (1971).
- [29] K. Kubodera, J. Delorme, and M. Rho, Phys. Rev. Lett. **40**, 755 (1978).
- [30] I.S. Towner, Nucl. Phys. A **542**, 631 (1992).
- [31] M. Kirchbach, D.O. Riska, and K. Tsushima, Nucl. Phys. A **542**, 616 (1992).
- [32] R. Schiavilla, R.B. Wiringa, V.R. Pandharipande, and J. Carlson, Phys. Rev. C **45**, 2628 (1992).
- [33] A. Kievsky, M. Viviani, and S. Rosati, Nucl. Phys. A **551**, 241 (1993).
- [34] A. Kievsky, M. Viviani, and S. Rosati, Nucl. Phys. A **577**, 511 (1994).

- [35] J. Carlson and R. Schiavilla, Rev. Mod. Phys. **70**, 743 (1998).
- [36] M. Kamimura, private communications.
- [37] N. Metropolis *et al.*, J. Chem. Phys. **21**, 1087 (1953).
- [38] J. Govaerts and J.-L. Lucio-Martinez, Nucl. Phys. A **678**, 110 (2000).
- [39] S.E. Kuhn *et al.*, Phys. Rev. C **50**, 1771 (1994).
- [40] R. Skibinski, J. Golak, H. Witala, and W. Glöckle, Phys. Rev. C **59**, 2384 (1999).
- [41] A. Kievsky *et al.*, Phys. Rev. C **58**, 3085 (1998).
- [42] M. Viviani, A. Kievsky, and S. Rosati, Few-Body Syst. **18**, 25 (1995).
- [43] M. Viviani, S. Rosati, and A. Kievsky, Phys. Rev. Lett. **81**, 1580 (1998).

TABLES

TABLE I. The values for the $N\Delta$ transition axial coupling constant g_A^* (in units of g_A), obtained by reproducing the experimental value of the Gamow-Teller (GT) matrix element in tritium β -decay with CHH wave functions corresponding to the AV18, AV14, AV18/UIX, and AV14/TM Hamiltonian models. The theoretical uncertainties are due to the experimental error with which the GT matrix element is known.

Interaction Model	g_A^*/g_A
AV18	1.25 ± 0.10
AV14	1.11 ± 0.09
AV18/UIX	1.17 ± 0.09
AV14/TM	1.04 ± 0.09

TABLE II. Binding energies in MeV of ^3He and ^3H calculated with the CHH method using the AV18, AV14, AV18/UIX, and AV14/TM Hamiltonian models. Also listed are the experimental values.

Interaction Model	^3He	^3H
AV18	6.917	7.617
AV14	7.032	7.683
AV18/UIX	7.741	8.473
AV14/TM	7.809	8.485
EXP	7.72	8.48

TABLE III. Capture rate Γ_0 in sec^{-1} , and angular correlation parameters A_v , A_t , and A_Δ , as defined in Eqs. (2.14)–(2.18), calculated using CHH wave functions corresponding to the AV18, AV14, AV18/UIX, and AV14/TM Hamiltonian models. The theoretical uncertainties, shown in parenthesis, reflect the uncertainty in the determination of the $N\Delta$ transition axial coupling constant g_A^* .

Observable	AV18	AV14	AV18/UIX	AV14/TM
Γ_0	1448(8)	1451(8)	1493(8)	1494(9)
A_v	0.5426(7)	0.5422(7)	0.5438(7)	0.5418(7)
A_t	-0.3520(18)	-0.3524(18)	-0.3525(17)	-0.3542(19)
A_Δ	-0.1054(19)	-0.1053(19)	-0.1038(18)	-0.1040(19)

TABLE IV. Cumulative contributions to the capture rate Γ_0 (in sec^{-1}) and angular correlation parameters A_v , A_t , and A_Δ . The CHH wave functions are obtained using the AV18/UIX Hamiltonian model. The column labeled “One-body” lists the contributions associated with the one-body vector and axial charge and current operators, while the column labeled “Mesonic” lists the results obtained by including, in addition, the contributions from meson-exchange mechanisms. Finally the column labeled “ Δ ” lists the results obtained by including also the Δ -excitation contributions, with g_A^*/g_A set to the central value of 1.17 (see Table I).

Observable	One-body	Mesonic	Δ
Γ_0	1316	1384	1493
A_v	0.5749	0.5511	0.5438
A_t	-0.3565	-0.3679	-0.3525
A_Δ	-0.0686	-0.0810	-0.1038

TABLE V. Cumulative contributions to the reduced matrix elements (RME’s) $C_0(V)$, $C_1(A)$, $L_1(A)$, $E_1(A)$, and $M_1(V)$. The CHH wave functions are obtained using the AV18/UIX Hamiltonian model. Note that $C_0(V)$ is purely real, while the other RME’s are purely imaginary. Notations as in Table IV.

RME	One-body	Mesonic	Δ
$C_0(V)$	0.3280	0.3277	
$C_1(A)$	-0.4076×10^{-2}	-0.4135×10^{-2}	-0.4397×10^{-2}
$L_1(A)$	0.2590	0.2618	0.2804
$E_1(A)$	0.5519	0.5563	0.5813
$M_1(V)$	-0.1128	-0.1314	-0.1355

TABLE VI. Capture rate Γ_0 (in sec^{-1}) and angular correlation parameters A_v , A_t , and A_Δ obtained with AV14/TM CHH wave functions, and only one-body operators (column labeled “One-body”) are compared with the results of Table 3 of Ref [10].

Observable	One-body	Ref. [10]
Γ_0	1287	1304
A_v	0.579	0.568
A_t	-0.351	-0.356
A_Δ	-0.070	-0.076

FIGURES

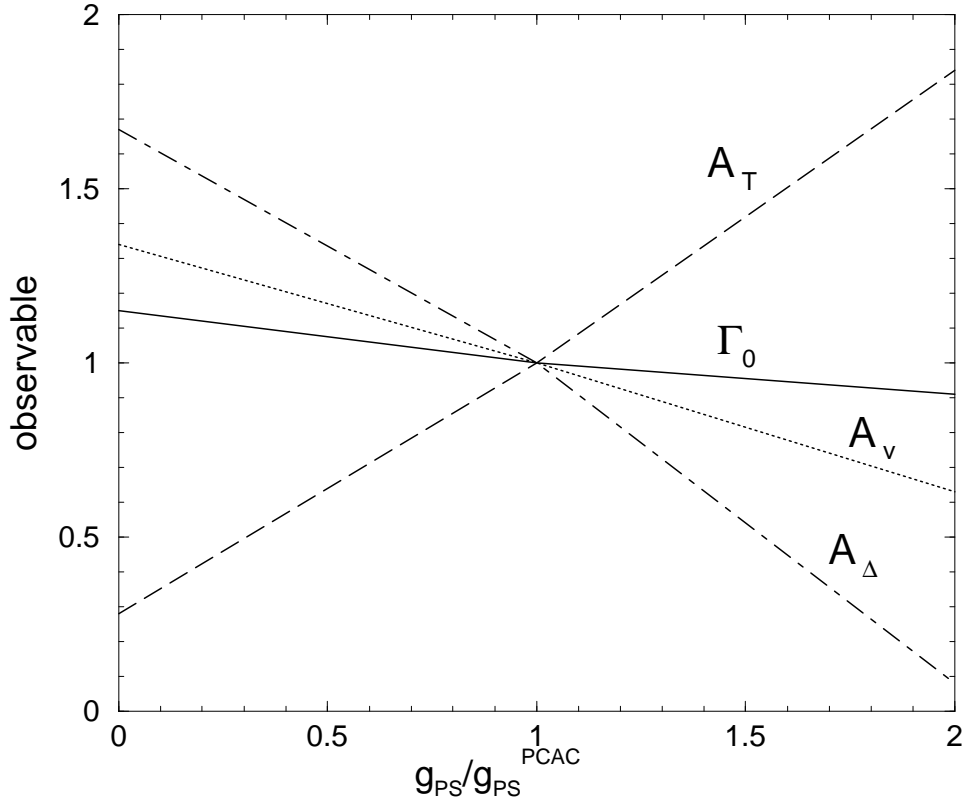


FIG. 1. Variation of the capture rate Γ_0 and angular correlation parameters A_v , A_t , and A_Δ with the induced pseudo-scalar coupling g_{PS} . The AV18/UIX CHH wave functions are used. For each observable, the ratio between the result obtained with the given value of g_{PS} and the PCAC prediction, listed in Table III, is plotted *versus* the ratio $g_{PS}/g_{PS}^{\text{PCAC}}$.